

Optical properties of charge-density-wave ground states for inversion layers in many-valley semiconductors

M. J. Kelly* and L. M. Falicov

Department of Physics, † University of California, Berkeley, California 94720

(Received 9 August 1976)

A charge-density-wave ground state satisfactorily accounts for the experimentally observed occupied valley degeneracy, high cyclotron mass and stress-dependent anisotropic conductivity in inversion layers at the Si(111)-SiO₂ interface. We make specific predictions about anisotropic optical transitions, the observation of which would distinguish the density-wave model from any alternative explanations of the experimental data.

I. INTRODUCTION

The observation of Shubnikov-de Haas oscillations corresponding to an occupied valley degeneracy of two^{1,2} in the *n*-type inversion layers at the Si(111)-SiO₂ interface is to be contrasted with the prediction of six by the self-consistent Hartree theory of Stern and Howard.³ The cyclotron effective mass¹ is also 20% higher than the theory predicts. We recently observed^{4,5} that a charge-density-wave (CDW) was the stable ground state of a two-dimensional unrestricted Hartree-Fock calculation for reasonable values of the important electron-electron interactions. This CDW accounts for the occupied valley degeneracy and the high cyclotron effective mass.

The *C*_{3_v symmetry of the Si(111) surface is reduced to a mere mirror symmetry which allows for three equivalent directions for the \vec{q} vector associated with the CDW. In a real sample, domains characterized by different \vec{q} vectors will be set up. Tsui and Kaminsky⁶ have measured the electrical conductivity of inversion layers at the Si(111)-SiO₂ interface and have found it to be isotropic. The application of uniaxial stress is accompanied by a marked anisotropy in the conductivity. Tsui and Kaminsky have interpreted this in terms of high-random-stress domains becoming aligned under the externally applied stress. The internal random stresses are set up by the bond mismatch at the interface, and they serve, via a deformation potential, to lift the valley degeneracy and account for the occupied valley degeneracy of two. The authors note that very large stresses must be invoked to reduce the occupied valley degeneracy. We would interpret the same data in terms of the growth of one CDW domain at the expense of the others under the external stress. The direction of large and small conductivity in the stressed sample is consistent with our "CDW β "}

ground state (Fig. 1) where four valleys are coupled into two pairs, each pair producing one occupied bonding band and one empty antibonding band. In this model, and using a simple inverse effective-mass argument, we would predict an anisotropic conductivity ratio of about 2:1 for a single CDW domain.

The existence of the antibonding bands is a feature of our model that comes directly from the correlation between electrons in different valleys. In this paper we examine in some detail the matrix elements and line shapes of optical transitions from the bonding to antibonding bands. We make specific predictions concerning the anisotropy and frequency dependence of the optical conductivity. Were the intervalley exchange interactions better known, we could make precise estimates of the threshold energies as a function of gate voltage. We confine ourselves to a parametrized calculation, noting that the observation of these optical transitions would serve both to distinguish our model from the random-stress model, and to put bounds on the various exchange interactions. Interband transitions have already been observed⁷ in the Si(100)-SiO₂ system, but these come from transitions to higher subbands. Our present transitions are comparable in oscillator strength, but the dipole matrix elements have a component in the surface plane, a feature peculiar to our model.

II. OPTICAL CONDUCTIVITY

We write⁸ the absorbing power *P* of the inversion layer of area *Q* in an electric field \vec{E} as

$$P = Q \langle \vec{E} \cdot \vec{\sigma}(\omega) \cdot \vec{E} \rangle, \quad (1)$$

where $\vec{\sigma}(\omega)$ is the long-wavelength limit of the two-dimensional frequency-dependent conductivity tensor. Using $\sigma_a = e^2/\hbar$ ($= 2.2 \times 10^9$ cm sec⁻¹) as a convenient atomic two-dimensional conductivity, we can write

$$\vec{\sigma}(\omega) = \sigma_a \frac{4\pi}{\hbar\omega} \left(\frac{\hbar^2}{2m} \right)^2 \frac{1}{Q} \sum_{nn'\vec{k}} f(\epsilon_n(\vec{k})) [1 - f(\epsilon_{n'}(\vec{k}))] \delta(\epsilon_{n'\kappa} - \epsilon_{n\kappa} - \hbar\omega) \langle \psi_{n'\kappa} | \vec{\nabla} | \psi_{n\kappa} \rangle \langle \psi_{n\kappa} | \vec{\nabla} | \psi_{n'\kappa} \rangle, \quad (2)$$

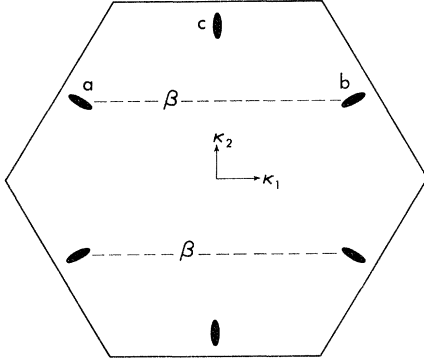


FIG. 1. Surface Brillouin zone for the Si(111) surface. CDW β ground state involves the \vec{q} vector labeled β .

where $\hbar\omega$ is the photon energy and the summation is over all bands of energies $\epsilon_{n\kappa}$, $\epsilon_{n'\kappa}$ within the first two-dimensional Brillouin zone. The Fermi occupation function $f(x)$ limits the contributions to the real excitations. In our present problem, $\psi_{n\kappa}$ is a wave function of energy $\epsilon_{n\kappa}$ in the occupied bonding band, while $\psi_{n'\kappa}$ is a corresponding antibonding wave function of energy $\epsilon_{n'\kappa}$. We confine ourselves to the study of the absorption line caused by the CDW ground-state to excited-state transition. Other transitions have comparable energies, but different physics governs both the oscillator strength and threshold as a function of gate voltage.

We obtained our CDW β ground state⁵ in terms of the effective-mass expansion $\epsilon_{a\kappa}$, $\epsilon_{b\kappa}$ of the two valleys which are coupled by the density wave, and the following four electron-electron interac-

tions: (i) V_1 , the intravalley direct interaction; (ii) U_1 , the intervalley direct interaction; (iii) $U_{2\alpha}$, the intervalley exchange interaction between valleys on the same $X\Gamma X$ axis of the bulk Brillouin zone, and (iv) $U_{2\beta}$, the same exchange interaction between "right-angle" valleys. With a number density of n electrons per unit area in the inversion layer of total area \mathcal{Q} , the energy bands are⁵

$$\epsilon_{n\kappa} = n\mathcal{Q} \left(\frac{3}{4}U_1 + \frac{1}{8}V_1 - \frac{1}{8}U_{2\alpha} - \frac{1}{4}U_{2\beta} \right) + \frac{1}{2}(\epsilon_{a\kappa} + \epsilon_{b\kappa}) - \left[\frac{1}{4}(\epsilon_{a\kappa} - \epsilon_{b\kappa})^2 + (U_1 + 2|U_{2\beta}|)^2 n^2 \mathcal{Q}^2 x^2 \right]^{1/2}, \quad (3)$$

and $\epsilon_{n'\kappa}$ is obtained with a plus sign before the square root. The x is a fraction of the form⁵

$$x = \frac{1}{8} - O((\epsilon_{a\kappa}/U_1)^2), \quad (4)$$

where the second term is a correction of order $(\epsilon_{a\kappa}/U_1)^2$. Equation (4) is derived from the self-consistent total energy minimization and, in the regions where CDW β is the stable ground state, $x \sim 0.10 - 0.12$. These bands are both doubly degenerate (see Fig. 1 for the two pairs of valleys), and there are two further empty nonbonding bands not involved in the density wave: these have an energy

$$\epsilon_{\kappa} = n\mathcal{Q} \left(U_1 - \frac{1}{2}U_{2\beta} \right) + \epsilon_{c\kappa}. \quad (5)$$

The wave functions are obtained as linear combinations of the valley wave functions. By defining

$$\Delta = (U_1 + 2|U_{2\beta}|) n\mathcal{Q} x, \quad (6)$$

and solving the secular equation explicitly

$$\psi_{n\kappa} = \frac{(2\lambda^{3/2}/\sqrt{\mathcal{Q}}) z e^{-\lambda z} e^{i\vec{\kappa} \cdot \vec{r}} \left[|\Delta| \phi_a(\vec{r}) e^{i\vec{p}_a z} + (\epsilon_{a\kappa} - \epsilon_{n\kappa}) \phi_b(\vec{r}) e^{i\vec{p}_b z} \right]}{[(\epsilon_{a\kappa} - \epsilon_{n\kappa})^2 + \Delta^2]^{1/2}}, \quad (7)$$

while $\psi_{n'\kappa}$ is the identical expression but with $\epsilon_{n'\kappa}$ instead of $\epsilon_{n\kappa}$ in the mixing coefficients. As in the Luttinger-Kohn⁹ approach, ϕ_a is the full Bloch function of the a th conduction-band minimum at \vec{k}_a , and λ^{-1} is the profile constant giving the overall width of the smooth envelope function.³⁻⁵ Here $\vec{\kappa} = (\kappa_1, \kappa_2)$ is a two-dimensional wave vector in the surface Brillouin zone, p_a and p_b are transverse longitudinal mass-mixing³ terms of the form $[-(\theta_{13}^a \kappa_1 + \theta_{23}^a \kappa_2)/\theta_{33}^a]$ for three-dimensional inverse effective mass tensor θ_{ij}^a for valley a .

With Eqs. (3) and (7), it is a straightforward exercise to evaluate Eq. (2). Before we do, we make a correction to the Luttinger-Kohn⁹ theory by amalgamating the two contributions $e^{i\vec{\kappa} \cdot \vec{r}}$ and $\phi_a(\vec{r})$ in Eq. (7) and replacing this by the full Bloch

function evaluated at $(\vec{k}_a + \vec{\kappa})$. Such a substitution is the first approximation to the interband contributions to the inversion layer wave function (omitted in the Luttinger-Kohn theory) and becomes more important as n increases. If we write the two-dimensional

$$\epsilon_{a\kappa} = \frac{\hbar^2}{2} \sum_{ij} \Theta_{ij}^a \kappa_i \kappa_j \quad (8)$$

with the mass-mixing corrections³⁻⁵ incorporated into the Θ , and if we note that

$$\Theta_{11}^a = \Theta_{11}^b, \quad \Theta_{22}^a = \Theta_{22}^b, \quad \Theta_{12}^a = -\Theta_{12}^b \quad (9)$$

for the valleys in Fig. 1, we find

$$\langle \psi_{n'\kappa} | \vec{\nabla} | \psi_{n\kappa} \rangle = \frac{i\Delta}{2 \left\{ \frac{1}{4} (\epsilon_{a\kappa} - \epsilon_{b\kappa})^2 + \Delta^2 \right\}^{1/2}} \times (2m\Theta_{12}^a \kappa_2, 2m\Theta_{12}^a \kappa_1, p_a - p_b), \quad (10)$$

where the z axis is normal to the surface. The Fermi occupation functions restrict the range of summation over $\vec{\kappa}$, or the integration via the standard

$$\sum_{\vec{\kappa}} - \frac{\mathcal{G}}{4\pi^2} \int d\vec{\kappa}.$$

The upper band is always empty, and the lower is full for $\vec{\kappa}$ within the Fermi distribution. Thus we have

$$\begin{aligned} \bar{\sigma}(\omega) &= 2\sigma_a \left(\frac{4\pi}{\hbar\omega} \right) \left(\frac{\hbar^2}{2m} \right)^2 \frac{1}{4\pi} \\ &\times \int d\kappa \delta(2(\hbar^4 \Theta_{12}^a \kappa_1^2 \kappa_2^2 + \Delta^2)^{1/2} - \hbar\omega) \\ &\times \langle \psi_{n'\kappa} | \vec{\nabla} | \psi_{n\kappa} \rangle \langle \psi_{n\kappa} | \vec{\nabla} | \psi_{n'\kappa} \rangle. \end{aligned} \quad (11)$$

The integration is over the occupied part of the bonding band. Since $\theta_{23}^a = \theta_{23}^b$ in our effective mass expansion, $p_a - p_b$ is proportional to κ_1 , and after some straightforward manipulation we obtain

$$\bar{\sigma}(\omega) = \sigma(\omega) \begin{bmatrix} \frac{|\Theta_{12}^a|}{\Theta_{22}^a} & 0 & 0 \\ 0 & \frac{|\Theta_{12}^a|}{\Theta_{11}^a} & \frac{1}{m\Theta_{11}^a} \frac{|\theta_{13}^a|}{\theta_{33}^a} \\ 0 & \frac{1}{m\Theta_{11}^a} \frac{|\theta_{13}^a|}{\theta_{33}^a} & \frac{1}{m^2\Theta_{11}^a |\Theta_{12}^a|} \left(\frac{\theta_{13}^a}{\theta_{33}^a} \right)^2 \end{bmatrix},$$

which in our case reduces to

$$\bar{\sigma}(\omega) = \sigma(\omega) \begin{pmatrix} 0.377 & 0 & 0 \\ 0 & 0.671 & 0.18 \\ 0 & 0.18 & 0.049 \end{pmatrix},$$

where

$$\begin{aligned} \sigma(\omega) &= \sigma_a \frac{2}{\pi} \frac{\Delta^2}{(\hbar\omega)^2 \left[\left(\frac{1}{2}\hbar\omega \right)^2 - \Delta^2 \right]^{1/2}} \\ &\times \left[\left(-|\Delta| + \frac{\hbar^2 n}{\nu m^*} + \frac{1}{2}\hbar\omega \right)^2 \right. \\ &\left. - \frac{\Theta_{11}^a \Theta_{22}^a}{\Theta_{12}^a} \left[\left(\frac{1}{2}\hbar\omega \right)^2 - \Delta^2 \right] \right]^{1/2}. \end{aligned} \quad (12)$$

In this last expression we have assumed that ν identical valleys of effective mass m^* are occupied, so that the Fermi level is at

$$E_F = n\mathcal{Q} \left(\frac{3}{4}U_1 + \frac{1}{8}V_1 - \frac{1}{8}U_{2\alpha} - \frac{1}{8}U_{2\beta} \right) - |\Delta| + \hbar^2 n / \nu m^*. \quad (13)$$

Equation (12) is our main result. $\sigma(\omega)$ is a two-dimensional conductivity of dimensions cm sec^{-1}

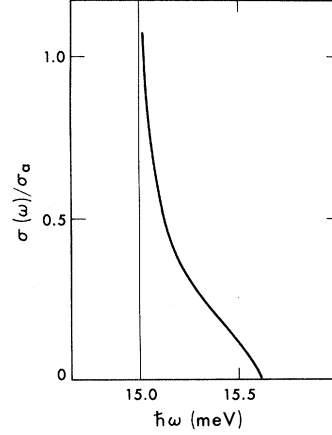


FIG. 2. Dimensionless optical absorption $[\sigma(\omega)/\sigma_a]$ from Eq. (12) for a typical set of parameters (the point marked * in Fig. 3) for $n = 4 \times 10^{12} \text{ cm}^{-2}$. Results are independent of $U_{2\alpha}$.

so that the computation of the dielectric constants requires an extra factor, being a typical inverse length in the third dimension, e.g., λ^{-1} .

III. DISCUSSION

(i) The optical absorption tensor [Eq. (12)] is valid for energies $\hbar\omega > 2|\Delta|$, at which energy there is a singular (inverse square root) threshold. The optical absorption vanishes for lower energies and also for energies greater than $\hbar\omega_1$, determined by the condition that the last factor in Eq. (12) vanishes. This latter condition describes the situation where the energy-conserving δ function [Eq. (2)] just fails to be satisfied for an occupied band state at the Fermi level.

(ii) The threshold at $2|\Delta|$ increases with gate voltage because n increases linearly with V_g ; U_1 and $U_{2\beta}$ also increase but more slowly with V_g . The cutoff at $\hbar\omega_1$ exhibits a slower dependence on V_g than does $2|\Delta|$. This is because the bonding-antibonding bands tend to get more parallel as the interaction term $|\Delta|$ increases. Although the Fermi distribution encompasses a greater area of $\vec{\kappa}$ space, the energy conserving δ function sweeps out the occupied portions of the bonding band even more rapidly. Of course, in the limit of $n \rightarrow \infty$, the bands are parallel, and in our present model a $\delta(\hbar\omega - 2|\Delta|)$ conductivity results. We thus expect to see an asymmetric line shape that narrows with increasing voltage.

(iii) In Fig. 2 we plot the line shape for a typical set of interaction values. Because of the uncertainties in the values of U_2 , we include in Fig. 3 the contours of threshold energy for the optical absorption on the assumptions that $n = 4 \times 10^{12} \text{ cm}^{-2}$, and that the electron-electron interactions are

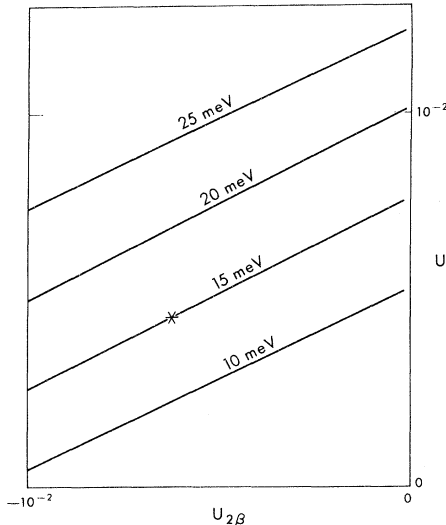


FIG. 3. Contours of constant threshold energy in the case where $n = 4 \times 10^{12} \text{ cm}^{-2}$ as a function of the interaction parameters. Role of $U_{2\alpha}$ is solely in determining the phase diagram (Refs. 4, 5) for the CDW β stability. The contours move almost linearly from the origin as functions of n and $(U_1 - 2U_{2\beta})$.

free parameters. These contours are independent of $U_{2\alpha}$, although the latter plays an important role in determining the phase diagram.^{4,5} The contours scale almost linearly with both $(U_1 - 2U_{2\beta})$ and n [to the extent that the corrections in Eq. (4) can be neglected].

(iv) From typical calculations we have performed, the linewidth decreases from ~ 0.8 to ~ 0.4 meV as $(U_1 + 2|U_{2\beta}|)$ increases from $\sim 0.5 \times 10^{-2}$ to 1.5×10^{-2} eV for a normalizing area $\mathcal{Q} = 10^{-12} \text{ cm}^2$ and with $n = 4 \times 10^{12} \text{ cm}^{-2}$.

(v) The theory could be generalized to include a relaxation time whose effect is to further broaden the line shape and mask the singularities in Eq. (12). The relaxation time should, however, be quite long at the cryogenic temperatures at which experiments are carried out.

(vi) We have calculated the integrated strength of the absorption line given by Eq. (12). We obtain

$$I \equiv \int \sigma(\omega) d\omega = \sigma_a \frac{2\Delta}{\hbar} Q, \quad (14)$$

where Q is a dimensionless number which depends on the parameters of the system. For the case discussed in Fig. 2,

$$Q = 0.02.$$

For the sake of comparison, we have calculated the integrated strength for transitions in the paramagnetic phase between the first subband and the first excited subband, with an envelope function which contains one nodal plane parallel to the sur-

face. In that case,

$$I = \sigma_a \omega_0 Q_0,$$

where $\hbar\omega_0$ is the energy difference between the bottoms of the two subbands and Q_0 is once again a dimensionless quantity. For typical values ($\hbar\omega_0 = 10$ meV, $n = 3.6 \times 10^{12} \text{ cm}^{-2}$, and $\lambda = 6 \times 10^{-2} \text{ \AA}^{-1}$),

$$Q_0 = 0.08,$$

i.e., a factor of 4 larger than the CDW case.

(vii) An important feature of our results is their polarization characteristics. The optical transition in the paramagnetic case is entirely in the \hat{z} direction, i.e., for electric fields perpendicular to the plane of the layer. As given in Eq. (12) above, the optical conductivity has both in-plane and out-of-plane contributions. Observation of the in-plane absorption would be a clear confirmation of the CDW β ground state.

(viii) Examination of the $\vec{\sigma}$ tensor clearly shows that its strength depends on the off-diagonal elements of the effective mass tensors θ_{ij} and Θ_{ij} . Charge-density waves arising from parallel ellipsoids ($\Theta_{ij} = 0$) would give no contribution, while charge-density waves arising from ellipsoids with a principal axis parallel to \hat{z} ($\theta_{13} = 0$) will give no absorption for an electric field in the \hat{z} direction, i.e., it will have only in-plane contributions.

(ix) The determinant of the $\vec{\sigma}$ tensor vanishes. This means that absorption can take place only with electric fields in a well-defined plane. The principal axes of the σ tensor are parallel to \hat{x} and to a direction in the $y\text{-}z$ plane tilted away from the \hat{y} direction. The direction of tilt depends on the longitudinal transverse mixing θ_{13} .

(x) The combined optical absorption of the metal, oxide, and bulk semiconductor would swamp the inversion-layer absorption in what would be the ideal geometry (light shone normal to the inversion layer). The use of polarized light in the geometry of Kamgar *et al.*¹⁰ could detect the absorption we have calculated. In a nonstressed multidomain sample, the absorption we have calculated would be isotropic, but under uniaxial stress the anisotropy of a single domain should dominate. With the restricted probe energies available, the asymmetric line shape will show up as the gate voltage causes the absorption peak to sweep through the fixed probe energy. It should be remembered that experimentally determined optical thresholds may be shifted in frequency by a variety of effects, including a shift to higher frequencies due to polarization effects.¹¹

Our calculation could also be carried through in a parallel manner for a spin-density-wave ground state.^{4,5} Similar results are achieved; elsewhere we have discussed the reasons^{4,5} why we believe

the CDW β solution to be the ground state.

In conclusion, we have made specific predictions about the line shape—its anisotropy, asymmetry, and linewidth—of the optical transitions between bonding and antibonding bands set up by a charge-density-wave ground state of the inversion layer at the Si(111)-SiO₂ interface. The detection of this

optical absorption would confirm our model of the many-valley semiconductor inversion layer electronic structure.

One of the authors (M.J.K.) wishes to acknowledge the support of the IBM Corporation through its Postdoctoral Fellowship Program.

*Permanent address: Cavendish Laboratory, Madingley Road, Cambridge CB3 0HE, England.

†Work supported in part by the National Science Foundation through Grant No. DMR72-03106-A02.

¹T. Neugebauer, K. Von Klitzing, G. Landwehr, and G. Dorda, *Solid State Commun.* **17**, 295 (1974).

²D. C. Tsui, *Bull. Am. Phys. Soc.* **21**, 334 (1976).

³F. Stern and W. E. Howard, *Phys. Rev.* **163**, 816 (1967); F. Stern, *Phys. Rev. B* **5**, 4891 (1972).

⁴M. J. Kelly and L. M. Falicov, *Phys. Rev. Lett.* **37**, 1021 (1976).

⁵M. J. Kelly and L. M. Falicov, preceding paper, *Phys. Rev. B* **15**, 1974 (1977).

⁶D. C. Tsui and G. Kaminsky, *Solid State Commun.* **20**, 93 (1976).

⁷D. C. Tsui and G. Kaminsky, *Phys. Rev. Lett.* **35**, 1468 (1975).

⁸M. J. Kelly and N. W. Ashcroft, *Phys. Rev. B* **8**, 2445 (1973).

⁹J. M. Luttinger and W. Kohn, *Phys. Rev.* **97**, 869 (1955).

¹⁰A. Kamgar, P. Kneschaurek, G. Dorda, and J. F. Koch, *Phys. Rev. Lett.* **32**, 1251 (1974).

¹¹W. P. Chen, Y. J. Chen, and E. Burstein, *Surf. Sci.* **58**, 263 (1976).